Int J Clin Exp Med 2016;9(3):5688-5698
www.ijcem.com /ISSN:1940-5901/IJCEM0020395

Original Article

Establishment and characterization of a new human oligosecretory myeloma cell line

Hiroyuki Yamazaki[1,3*], Shogo Tajima[2*], Takahiro Takeuchi[1]

Departments of [1]Hematology, [2]Pathology, Shizuoka Saiseikai General Hospital, Shizuoka, Japan; [3]Department of Hematology and Oncology, Graduate School of Medicine, Kyoto University, Kyoto 606-8507, Japan. [*]Equal contributors.

Received November 23, 2015; Accepted February 10, 2016; Epub March 15, 2016; Published March 30, 2016

Abstract: Multiple myeloma is a neoplasm derived from abnormal plasma cells exhibiting excessive proliferation either within or outside of the bone marrow. While the majority of myelomas are classified into distinct types based on the production of different classes of immunoglobulins, a small percentage of these tumor cells fail to exhibit immunoglobulin secretion and are classified as nonsecretory myelomas. The nonsecretory type is further subdivided into the intracytoplasmic immunoglobulin producer and nonproducer types. Notably, recent studies detected a novel form of myeloma, oligosecretory myeloma, which comprises a portion of the nonsecretory type. While the prevalence of the oligosecretory type increases with disease progression, the mechanism underlying the development of these cells remains unclear. Likewise, oligosecretory myeloma cell lines remain rare. Here, we describe the development of a new myeloma cell line, designated THK-72, from the pleural effusion of a myeloma patient initially diagnosed with IgG kappa type myeloma, which subsequently transformed to oligosecretory myeloma. THK-72 cells proliferated in single suspension culture without any feeder layer or IL-6 supplementation, and no immunoglobulin secretion was detected in the supernatant of these cells by immunoelectrophoresis analysis. Morphological analyses indicated that THK-72 cells had plasmacytoid appearance, while PCR and flow cytometry analyses demonstrated that the cells were negative for B-cell marker and EBV-infection, thereby indicating that THK-72 comprises a "true" myeloma cell line. Interestingly, contrary to the bortezomib resistance observed during the clinical course, the THK-72 cells were sensitive to bortezomib *in vitro*. As THK-72 arose from a classical myeloma, this oligosecretory myeloma cell line will be useful for studies regarding the biological nature of plasma cell neoplasms.

Keywords: Oligosecretory myeloma, human myeloma cell line, bortezomib

Introduction

Multiple myeloma is characterized by the expansion of malignant plasma cells within the bone marrow and/or extramedullary. These malignant plasma cells secrete abnormal immunoglobulins causing a monoclonal gammopathy that can be identified in the serum and/or urine by immunoelectrophoresis. Based on their immunoglobulin (Ig) components, classical myelomas are classified into the IgG, IgA, IgE, IgD, IgM, or null (namely, Bence-Jones protein type) heavy chain type and the kappa or lambda light chain type. However, in approximately three per cent of multiple myeloma cases, no immunoglobulins can be detected. Such myelomas are classified as the nonsecretory type [1]. Nonsecretory myelomas are further subdivided into the intracytoplasmic immunoglobulin producer type (also referred to as the true nonsecretory type), in which immunoglobulins are synthesized in plasma cells but not excreted into blood, and the nonproducer type, in which immunoglobulins are absent from plasma cells [2-4].

In the early 2000 s, the development of a sensitive assay aimed at evaluating the levels of serum free light chain (sFLC) [5] enabled the detection of minimal amounts of abnormal immunoglobulin secretion in a portion of nonsecretory producer type myelomas. This group was subsequently newly categorized as oligosecretory myeloma. Recent reports indicate that oligosecretory myeloma accounts for approximately 10% of patients with newly diagnosed

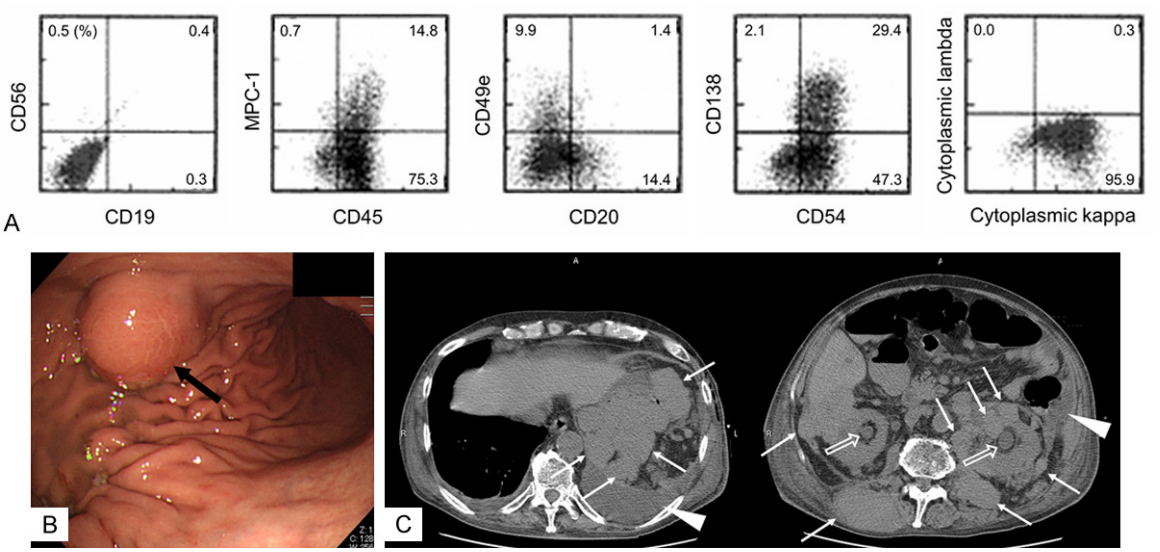

Figure 1. Clinical analysis of the patient. A. Flow cytometry analysis of the bone marrow specimen harvested at the initial diagnosis. B. Gross findings regarding the stomach, as determined by upper gastrointestinal endoscopy. Black arrow indicates a plasmacytoma presenting as a submucosal tumor. C. Computed tomographic scanning of the patient's body: white arrows indicate plasmacytomas; white arrow heads indicate pleural effusions or ascites; the hollow arrow indicates a hydroureter caused by urinary tract obstruction due to multiple plasmacytomas within the abdomen.

myeloma, and that this prevalence increases with advanced disease progression [6, 7]. Similarly, several recent studies indicated a cellular basis for serological M-protein changes during disease relapse [8, 9]. However, the molecular mechanisms underlying this phenomenon and the association between disease progression and immunoglobulin alteration remain to be elucidated. While human myeloma cell lines are useful for studying the biology of multiple myeloma, oligo- and nonsecretory myeloma cell lines remain rare [10-12].

In this paper, we present the case of an oligosecretory myeloma patient who was initially diagnosed with IgG kappa type myeloma. The patient exhibited systemic multiple plasmacytomas, indicating multiple drug resistance, including resistance to bortezomib, at recurrence. We subsequently developed and characterized a new oligosecretory myeloma cell line, designated THK-72, from pleural effusion harvested from the patient during the progressive stage of the disease. To date, several molecular mechanisms for the acquisition of bortezomib resistance have been reported, including the development of somatic mutations in proteasome subunit β type-5 (*PSMB5*) [13], and protection by particular bone marrow mesenchymal stem cells [14]. Nevertheless, our findings intimate that there is another mechanism for gaining drug resistance, independent of intrinsic mutations or the bone marrow milieu, which occurs *in vivo*.

Materials and methods

Case history

A 68-year-old man admitted to Shizuoka Saiseikai General Hospital in February 2009 with lumbocostal pain was diagnosed with IgG kappa type myeloma along with sacral plasmacytoma. Serum immunoglobulin levels on admission were as follows: IgG, 4,625 mg/dL; IgA, 25 mg/dL; IgM, 20 mg/dL; IgD, 0.6 mg/dL. The presence of monoclonal IgG kappa proteins in the serum were confirmed by electrophoretic examination, and Bence-Jones protein was detected in the patient's urine. The serum levels of albumin and β2 microglobulin were 3.8 mg/dL and 3.6 μg/mL, respectively. Flow cytometry analysis revealed that 70% of monoclonal plasma cells in the patient's bone marrow had kappa light chain restriction. The phenotype of these aberrant blasts was $CD19^{-}CD20^{-}CD56^{-}$, $MPC\text{-}1^{low}CD49e^{-}$, which is indicative of immature myeloma cells (**Figure 1A**). The patient was administered a cycle of melphalan (L-PAM) and prednisolone. These treatments, combined with radiotherapy of the vertebrae and administration of bortezomib and thalido-

mide, led to partial remission (the serum IgG level decreased to 881 mg/dL). Subsequently, the patient received high-dose L-PAM chemotherapy with autologous peripheral blood stem cell transplantation (auto-PBSCT). Eleven months after diagnosis he developed a plasmacytoma on the right chest wall and pleuritis carcinomatosa; however, there was no elevation in serum IgG levels, and mature plasma cells were absent from the bone marrow. sFLC assay and immunofixation analyses could not be performed due to the lack of insurance coverage in Japan at the time. A combination of local radiotherapy, bortezomib, thalidomide, and dexamethasone treatment was again administered, but progressive disease resulted. A second round of high-dose cyclophosphamide chemotherapy with auto-PBSCT and combination therapy with bortezomib, lenalidomide, and dexamethasone was also ineffective. The patient died 16 months after diagnosis and exhibited widespread plasmacytomas in the lung, pleura, peritoneum, diaphragm, stomach, liver, pancreas, intestine, kidney, bladder, bone, and skin, including the scalp, as determined by endoscopic examination and computed tomography analysis (**Figure 1B**, **1C**). A slight elevation in serum IgG levels (1,828 mg/dL) was observed in extremis.

Cell culture

A month before his death, the patient was subjected to pleural effusion aspiration, and poorly differentiated myeloma cells were identified in the resulting fluid via histology and flow cytometry analyses. Mononuclear cells were isolated using Ficoll-Paque PLUS reagent (GE Healthcare, Little Chalfont, UK), resuspended in RPMI 1640 medium (Thermo Fisher Scientific, Waltham, MA, USA) supplemented with 20% fetal bovine serum (FBS), 100 U/mL penicillin, 100 μg/mL streptomycin, and 250 ng/mL amphotericin B (Wako Pure Chemical Industries, Ltd., Osaka, Japan), and cultured in a humidified incubator at 37°C with 5% CO_2. For early passages, cells were also cultivated in MarrowMax medium (Thermo Fisher Scientific). Lastly, RPMI 1640 medium supplemented with 10-20% FBS was utilized for growth curve and growth inhibition assay analyses.

Morphological studies

Clots of cells from the established cell line were subjected to Hematoxylin-Eosin and immunohistochemical staining and observed microscopically. For transmission electron microscopy analyses, harvested cells were initially fixed in suspension with 2.5% glutaraldehyde and 2% paraformaldehyde for 2 hours at 25°C, and were postfixed in 1% OsO_4 for 2 hours at 4°C. The cells were then dehydrated through a graded series of ethanol, treated with N-butyl glycidyl ether (QY-1), embedded in Epon 812 resin (TAAB Laboratories Equipment, Berks, UK), and cut into ultrathin (60-nm) sections using an Ultracut-J (Reichert, Vienna, Austria) ultramicrotome. Sections were stained with Reynold's lead citrate and uranyl acetate, and examined with a JEM-1200EX electron microscope (JEOL, Ltd, Tokyo, Japan).

Immunohistochemical analyses of immunoglobulins

The subcellular localization of immunoglobulin components, i.e. IgG, IgA, and IgM heavy chains, and lambda and kappa light chains, in cultured cells was determined via immunohistochemical analysis using the labeled streptavidin biotin method. For these analyses, cells were stained with anti-IgG, anti-IgA, anti-IgM, anti-kappa, or anti-lambda rabbit polyclonal antibodies and visualized using an I-VIEW DAB Universal Kit (Roche, Tokyo, Japan).

Immunoelectrophoretic analysis

THK-72 cells were cultivated for 2 weeks. The culture supernatant was then harvested and separated by 1% agarose gel electrophoresis. The resulting gel was then treated with anti-human whole serum, anti-IgG, anti-IgA, anti-IgM, anti-lambda antibodies, and anti-kappa antisera for 13 hours at 19°C, washed with buffered saline, and stained with Coomassie Blue R-250.

Immunophenotype analysis

Approximately 5.0 × 10^4 THK-72 cells were suspended in PBS with 0.2% bovine serum albumin (BSA) and incubated with 5 μg/mL anti-human antibody at 4°C for 20 minutes. The cells were then washed with PBS and subjected to flow cytometry analysis. Cytoplasmic immunoglobulins were stained with fluorescein-conjugated anti-immunoglobulin antisera after cell fixation. The stained cells were analyzed using a FACScan flow cytometer (BD Biosciences, San Jose, CA, USA). The following cell surface or cytoplasmic markers were

detected using the corresponding antibody: cluster of differentiation 7 (CD7), using 3A1-RD1 (Beckman Coulter, Inc., Brea, CA, USA); CD19, using CD19-IO-Test-FITC (Beckman Coulter); CD20, using B-Ly1-FITC (Dako Denmark A/S, Glostrup, Denmark); CD33, using CD33-FITC (Dako Denmark A/S); CD38, using CD38-R Phycoerythrin Cyanin 5.1 (CD38-PC5; Immunotech, Marseille, France); CD45, using CD45-peridinin chlorophyll-alpha protein (CD45-Per-CP, BD Biosciences); CD49e, using CD49e-PE (BD Biosciences); CD54, using ICAM-1-FITC (Dako Denmark A/S); CD56, using NKH-1-RD1 (Beckman Coulter); CD138, using CD138-IO-Test-PE (Immunotech); human leukocyte antigen (HLA)-DR, using Anti-HLA-DR-FITC (BD Biosciences); mature plasma cell-1 (MPC-1), using MPC-1-RPE (Otsuka Pharmaceutical Co, Ltd., Tokyo, Japan); and immunoglobulin light chains, using kappa-FITC and lambda-RPE (Dako Denmark A/S).

Chromosomal analysis

Chromosomal analysis using a G-banding approach was performed on cells at the 12th passage. Briefly, THK-72 cells were treated with 0.05 μg/mL colcemid for 8 hours, washed with PBS, and suspended in a hypotonic solution (0.075 M potassium chloride). Cells were then fixed by dilution in Carnoy's fixative glacial acetic acidimethanol (1:3) and incubation for 30 min. The cells were aliquoted onto glass slides in air-dried preparations, stained with Giemsa solution, mounted, and photographed for counting. Ten cells in metaphase were analyzed per slide. The cytogenetic nomenclature used to describe the results followed the recommendations of the International System for Human Cytogenetic Nomenclature (ISCN 2009).

EBV detection

DNA was extracted from harvested cells using a QIAamp DNA Blood Mini kit (Qiagen, Venlo, Netherlands). EBV infection was determined by PCR analysis using an EBV-specific primer set, as previously described [15].

Quantification of IL-6

The level of IL-6 in the supernatants of cultured cells was measured via a chemiluminescent enzyme immunoassay (CLEIA) technique [16] using a two-step sandwich method with a cartridge for IL-6 measurement (a Human IL-6 CLEIA Fujirebio, Fujirebio, Tokyo, Japan). Briefly, the IL-6 binds to both the ferrite-labeled antibody and alkaline phosphatase-conjugated antibody and forms an immune complex after incubation for 10 minutes at 37°C. After magnetic separation of the particles, an enhanced luminol/peroxide substrate solution containing 3-(2'-spiroadamantane)-4-methoxy-4-(3'-phosphoryloxy)-phenyl-1, 2-dioxetane disodium salt was added and further incubated for 5 min at 37°C. Then, the chemiluminescence was measured using a Lumipluse 1200 photon counter (Fujirebio). The lower detection limit for serum IL-6 was 0.1 pg/mL.

Growth curve and growth inhibition assay

Approximately 5.0×10^4 THK-72 cells/well were aliquoted into 6-well plates. The number of cells in each well was counted sequentially via the trypan blue dye exclusion method, and doubling times were determined by generating a growth curve. The inhibitory effect of bortezomib (Janssen Pharmaceutica, Beerse, Belgium), doxorubicin (Novartis, Basel, Switzerland), and vincristine (Nippon Kayaku, Tokyo, Japan) on the growth of THK-72 cells was then assessed. For the sensitivity of THK-72 cells to bortezomib, the median inhibitory concentration (IC50) was computed using the XLfit 4.2 add-in software for Excel. Experiments were performed in triplicate.

Statistical analyses

Mann-Whitney *U* test was used to evaluate differences between two groups in the growth curve and inhibition analyses. P values < 0.05 were considered statistically significant.

Results

Establishment of the THK-72 cell line

A few days after establishing the primary culture, round cells were observed to proliferate in single suspension without forming cell clumps. This cell line grew continuously and has been maintained for over 18 months. Furthermore, the cells, which have been designated THK-72, were successfully revived after storage in liquid nitrogen.

Morphological appearance of THK-72 cells

Analysis of the myeloma cells from the patient's bone marrow specimen (**Figure 2A**) and the pleural effusion specimen (**Figure 2B**), harvested at the initial diagnosis and at recurrence, respectively, detected plasmablasts with typi-

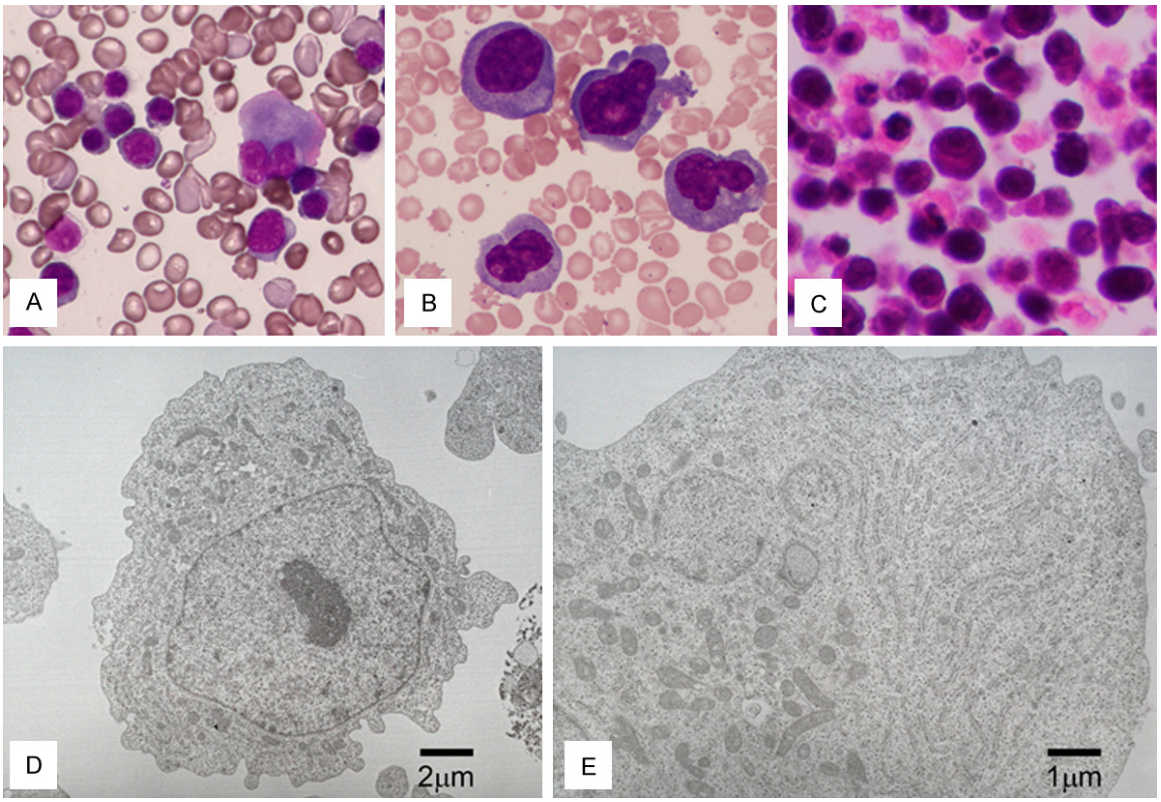

Figure 2. Cytologic appearance of the original blasts and the THK-72 cells. (A) Microscopic images of myeloma cells in the bone marrow aspirate and the (B) pleural effusion obtained from the patient after Wright-Giemsa staining (magnification, 400×). (C) Microscopic image of the block of THK-72 cells after Hematoxylin-Eosin staining (magnification, 100×). (D, E) Electron microscopic images of THK-72 cells after uranyl acetate and lead citrate staining [magnification, 3,000× (D) and 6,000× (E)].

cal myeloma cell morphologies, including basophilic cytoplasm, eccentric perinuclear halos, and eccentric nuclei. Furthermore, polylobulated nuclear and multinuclear cells were often observed in the pleural effusion sample. Similarly, THK-72 cells exhibited a deeply basophilic cytoplasm, high nuclear-to-cytoplasmic ratios, and eccentric nuclei containing prominent nucleoli and mitoses (**Figure 2C**). In addition, electron microscopy analyses demonstrated that the cells exhibited a typical plasmacytoid appearance, and that the cytoplasm contained numerous mitochondria and a well-developed rough endoplasmic reticulum in paralleled stacks (**Figure 2D**, **2E**).

Expression and secretion of immunoglobulins by THK-72

THK-72 cells exhibited light chain restriction; they were positive for kappa cytoplasmic staining (**Figure 3A**), and negative for lambda staining (**Figure 3B**). Among the immunoglobulin heavy chains, THK-72 were positive for IgG (**Figure 3C**), but negative for IgA (**Figure 3D**) and IgM (**Figure 3E**). Meanwhile, as shown in **Figure 3F**, immunoelectrophoretic analysis using anti-human whole serum antibody failed to detect any immunoglobulins, including IgG and κ chain, in the culture supernatant of THK-72 cells. The sensitivity of this method is > 5 mg/dL [17]. As such, these results indicate that little, if any immunoglobulins were secreted from THK-72 cells.

Immunophenotype analysis

Similar to the cells harvested from the patient's bone marrow upon initial diagnosis (**Figure 1A**), both the cells collected directly from the pleural carcinomatosa and the THK-72 cell line were positive for CD54 (84.8%), CD138 (79.6%), kappa immunoglobulin (97.3%), and HLA-DR (90.5%); slightly positive for CD45 (63.6%); and negative for CD7, CD19, CD20, CD33, CD49e, CD56, and MPC-1. This $CD19^{-}CD20^{-}CD56^{-}$ and $MPC\text{-}1^{-}CD49e^{-}CD45^{+/-}$ phenotype combined with negative indications for B- and T-cell mark-

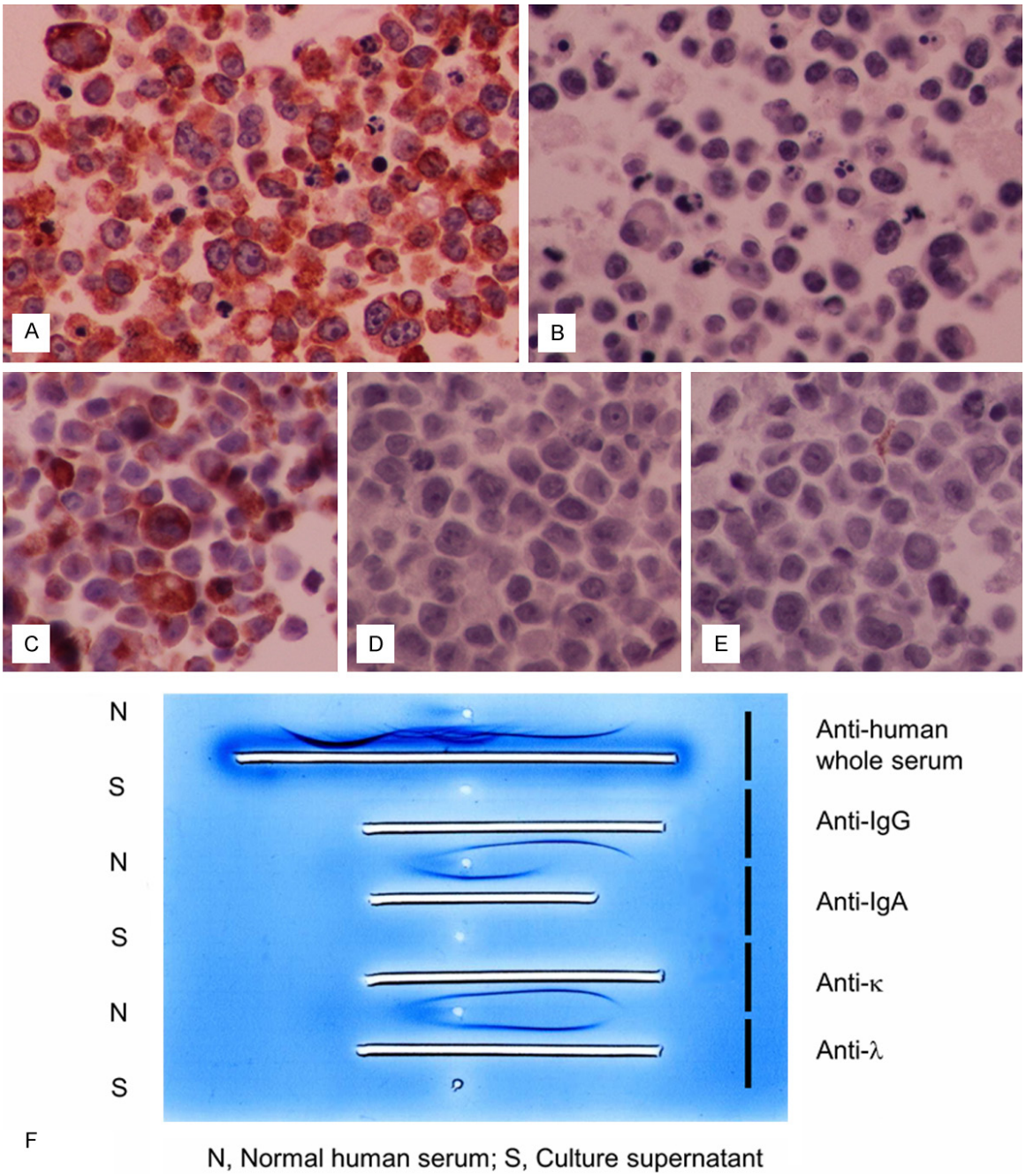

Figure 3. Immunogloblin expression and secretion in THK-72 cells. (A-E) THK-72 cells were subjected to the avidin-biotin/immunoperoxidase staining technique using the following antibodies: anti-kappa (A), anti-lambda (B), anti-IgG (C), anti-IgA (D), and anti-IgM (E). (F) Immunoelectrophoresis assay analysis of culture supernatant harvested from THK-72 cells. Normal human serum was used as a positive control.

ers indicated that the THK-72 cell line was comprised of immature myeloma cells [18, 19].

Chromosomal analysis

Chromosomal analysis of THK-72 cells revealed a hyperdiploid karyotype with a unimodal chromosome number of 50 (**Figure 4**). Furthermore, the following structural and numerical karyotype abnormalities were identified in nine of the ten cells examined: derivative chromosomes, der(Y)t(Y;1)(q12;q21), der(6)t(1;6)(q12;q13)x2, and der(7)t(7;12)(p22;q22); a chromosomal translocation, t(7;12); an interstitial deletion

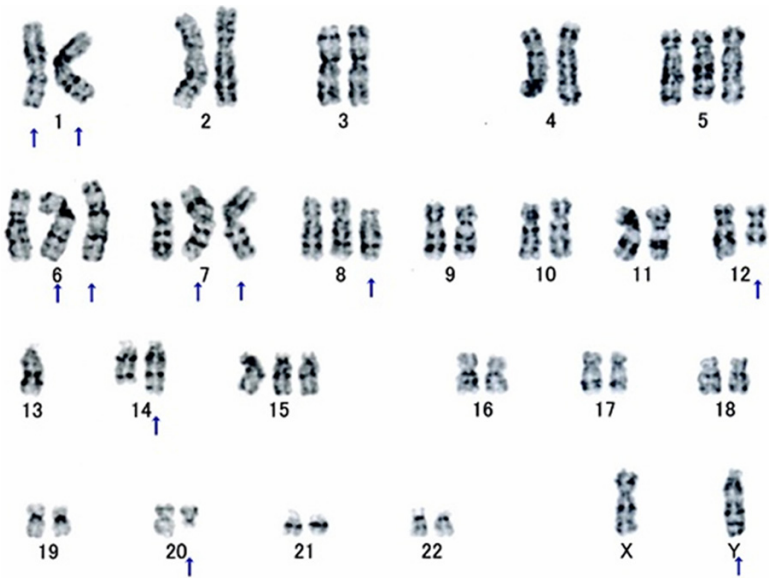

Figure 4. Giemsa-banded karyotype of THK-72. The following major cytogenetic abnormalities were identified: 50, X, der(Y)t(Y;1)(q12;q21), add(1)(q21), +5, +6, der(6)t(1;6)(q12;q13)x2, +der(7)t(7;12)(p22;q22), t(7;12), +add(8)(p11.2), -13, add(14)(q32), +15, del(20)(q11.2q13.3).

within chromosome 20, 20(q11.2q13.3); and additional chromosomes, 1q21, 8p11.2, and 14q32; trisomy, 5, 6, and 15; monosomy, 13. Lastly, an interstitial deletion of chromosome 1p was observed in only one of the ten cells examined, which intimated that the abnormality was derived from the stem cell line or was an artifact.

EBV detection

EBV DNA was not detected in THK-72 cells by PCR analysis (data not shown).

Secreted IL-6 in culture supernatant

No IL-6 was detected in the culture supernatant of THK-72 cells (data not shown).

Growth curve analysis and growth inhibition using anticancer drugs

THK-72 cells exhibited constant proliferation in RPMI 1640 supplemented with 10-20% FBS, with a doubling time of approximately 40-80 hours. However, various anticancer drugs effectively inhibited the growth of these cells *in vitro*. Specifically, while treatment with 10 ng/mL bortezomib, vincristine, or doxorubicin resulted in a significant reduction in the growth of THK-72 cells (**Figure 5A**), bortezomib had the most dramatic cytotoxic effect on THK-72 cells. To investigate the sensitivity of our myeloma cell line to bortezomib, THK-72 cells were treated with a range of concentrations of the agent. As shown in **Figure 5B**, at concentrations greater than 1 ng/mL, bortezomib exhibited time-dependent cytotoxity. The IC50 value of bortezomib for THK-72 cells was calculated as 3.31 ng/mL (**Figure 5C**).

Discussion

According to the international staging system (ISS) for multiple myeloma, the patient described in this study presented with stage II myeloma at the initial diagnosis; however, he then followed a rapid progressive course. During the terminal stage, bone marrow examination failed to detect myeloma cells, whereas systemic extramedullary plasmacytomas developed extensively. The observed decrease in CD56, CD49e, and CD45 expression may have been associated with the widespread extramedullary expansion and disease acceleration in this patient [20]. Chromosomal aberrations also relate prognostic importance. Indeed, the chromosome 1q21 amplification and monosomy 13 encoded by the THK-72 cells are the most important chromosomal aberrations associated with poor outcomes [21, 22]. Lastly, karyotypic instability is often observed in progressive myeloma [23], which is consistent with the clinical course of the patient described here.

The patient demonstrated a prominent decrease in immunoglobulin production at relapse. In view of current knowledge, although sFLC assay and immunofixation analyses could not be performed, it was reasonable to consider the patient's pathological condition a transformation to oligosecretory myeloma rather than to nonsecretory myeloma. Alterations in immunoglobulin levels accompanying disease progression have been reported in several publications, and oligosecretory myeloma is more frequently observed with advanced disease pro-

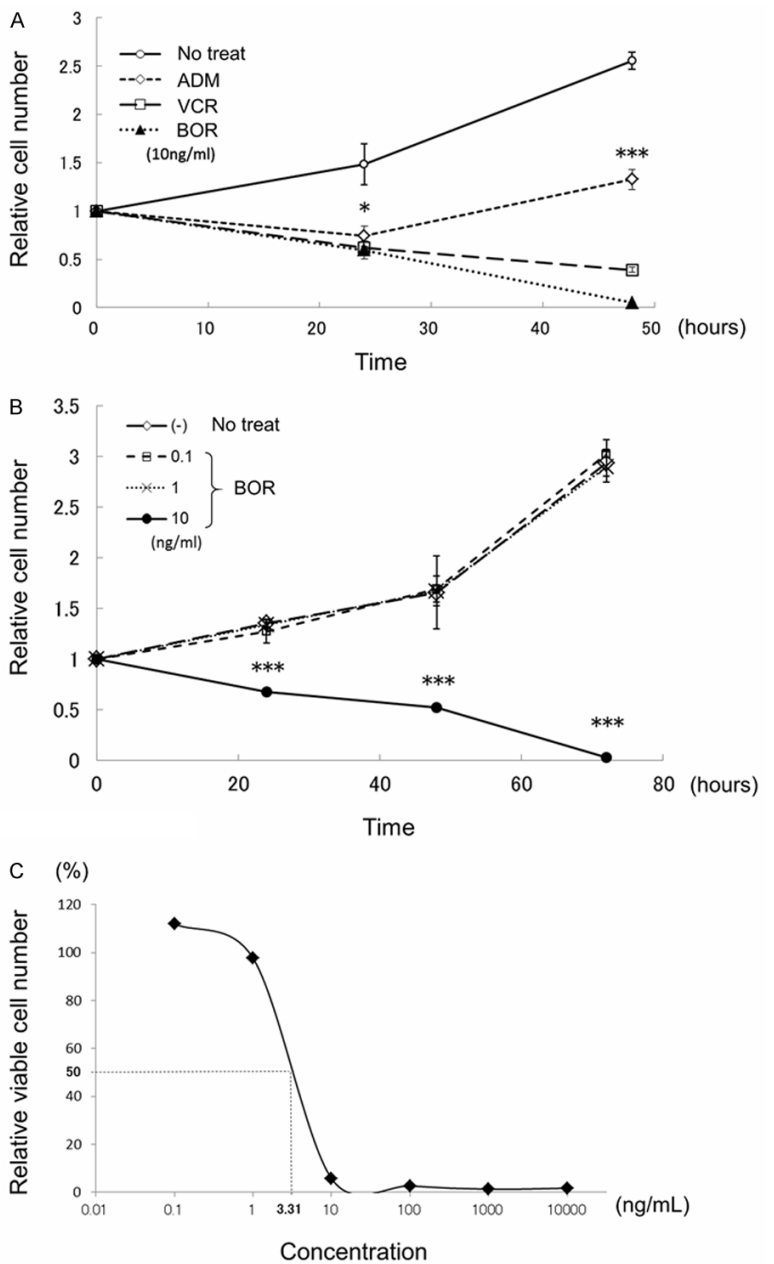

Figure 5. Effect of anticancer agents on THK-72 cells. A. Graphic depiction of the growth rate of THK-72 cells incubated with bortezomib (10 ng/mL), vincristine (10 ng/mL), or doxorubicin (10 ng/mL). B. Graphic depiction of the growth rate of THK-72 cells treated with 0.1, 1, and 10 ng/mL bortezomib. C. Graphic depiction of the number of viable THK-72 cells after treatment with a range of concentrations (0.1-10 μg/mL) of bortezomib for 48 hours. The median inhibitory concentration (IC50) value of bortezomib for THK-72 cells was 3.31 ng/mL. Relative cell number values were calculated as the proportion of cell counts to the initial value. Asterisks indicate a statistically significant difference from the control cells; *P < 0.05, ***P < 0.001.

gression [7]. Similarly, other studies detected a conversion in serological M-protein levels at disease relapse, which defined the emergence of a de-differentiated clone of light or heavy chain-only producing cells, and is referred to as immunoglobulin "escape" [8, 9, 24]. Currently, sFLC assay or serum immunoglobulin measurements are used to monitor treatment response and disease progression in myeloma patients. In addition, we emphasize the importance of monitoring immunoglobulin escape and to assess patient status via multimodal inspections. While the molecular mechanisms underlying these immunoglobulin alterations are poorly understood, studies of nonsecretory myeloma may help to shed light on these processes. Analysis of a nonsecretory myeloma clinical sample detected the production of abnormal light chains, which resulted from the acquisition of a frameshift mutation within the sequence encoding the constant region of the molecule [3]. In addition, exon skipping of mutations in the altered variable region has been shown to lead to production of abnormal immunoglobulin chains [25]. These abnormalities can induce misfolding of the encoded light chain protein, resulting in targeting for proteasome-mediated degradation [26].

In this study, we established the THK-72 cell line from the pleural effusion harvested from a patient presenting with terminal oligosecretory myeloma. Negative indications of B-cell markers and EBV infection indicate that THK-72 cell line is not a transformed B-lymphoblastoid cell line, but instead comprises a "true" human myeloma cell line [27]. Similar to the original myeloma cells harvested from the patient at relapse, THK-72 cells secreted little monoclonal IgG

kappa protein into the culture supernatant. Considering the rarity of nonsecretory myeloma cell lines [10-12], additional analyses of the THK-72 cell line should provide further information regarding oligo- or nonsecretory myelomas that are derived from the classical type.

Five bortezomib-resistant myeloma cell lines have been previously established *in vivo* or *in vitro* [28-31]. While the IC50 values of bortezomib for sensitive myeloma cell lines are approximately 1-15 ng/mL, those for bortezomib-resistant cell lines are greater than 20 ng/mL. In a previous study, Ri et al. (2010) reported a bortezomib-resistant myeloma cell line that encodes an amino acid substitution (G322A) within the PSMB5 that inhibits bortezomib from binding to the proteasome [13]. Meanwhile, other studies have demonstrated that particular bone marrow mesenchymal stem cells or stromal cells protect myeloma cells from bortezomib-induced apoptosis through the β-catenin signaling pathway or the NF-κB pathway [14, 32]. Notably, contrary to the patient's clinical course, the THK-72 cell line exhibited sensitivity to bortezomib. We cannot exclude the possibility of expansion only from bortezomib-sensitive clones; however, THK-72 cells were established without bortezomib selection. Given that myeloma cells were absent from the bone marrow aspirate and abundant in the extramedullary of this patient during the terminal stage, the bone marrow microenvironment likely played little role in the acquisition of drug resistance by the myeloma cells in his body. These facts suggest that, in addition to the development of mutations within the proteasome and alterations in the bone marrow milieu, there is another, as yet undescribed, mechanism for acquiring bortezomib-resistance. As such, further exploration of drug-resistance in myeloma is needed to characterize this process.

Acknowledgements

We thank Kimihiko Yamada for his help and support with the ultrastructual studies. We also thank Michihiko Waki for his helpful comments. We acknowledge the SRL Co. Research Service (Tokyo, Japan) for technical assistance regarding the chromosomal analyses, immunoelectrophoresis, FCM, EBV DNA examination, and IL-6 measurements.

Disclosure of conflict of interest

None.

Address correspondence to: Dr. Hiroyuki Yamazaki, Department of Hematology and Oncology, Graduate School of Medicine, Kyoto University, 54 Shogoin Kawahara-cho, Sakyo-ku, Kyoto 606-8507, Japan. Tel: +81-75-751-4964; Fax: +81-75-751-4963; E-mail: ymzkhryk@kuhp.kyoto-u.ac.jp

References

[1] Kyle RA, Gertz MA, Witzig TE, Lust JA, Lacy MQ, Dispenzieri A, Fonseca R, Rajkumar SV, Offord JR, Larson DR, Plevak ME, Therneau TM and Greipp PR. Review of 1027 patients with newly diagnosed multiple myeloma. Mayo Clin Proc 2003; 78: 21-33.

[2] Mancilla R and Davis GL. Nonsecretory multiple myeloma. Immunohistologic and ultrastructural observations on two patients. Am J Med 1977; 63: 1015-1022.

[3] Coriu D, Weaver K, Schell M, Eulitz M, Murphy CL, Weiss DT and Solomon A. A molecular basis for nonsecretory myeloma. Blood 2004; 104: 829-831.

[4] Chen W, Namara MM, Kim Y and Huang Q. t(11;14) Plasma cell disorder presents as a true nonsecretory, nonproducer multiple myeloma. Clin Lymphoma Myeloma 2009; 9: 243-246.

[5] Drayson M, Tang LX, Drew R, Mead GP, Carr-Smith H and Bradwell AR. Serum free light-chain measurements for identifying and monitoring patients with nonsecretory multiple myeloma. Blood 2001; 97: 2900-2902.

[6] Barlogie B, Alexanian R, Pershouse M, Smallwood L and Smith L. Cytoplasmic immunoglobulin content in multiple myeloma. J Clin Invest 1985; 76: 765-769.

[7] Larson D, Kyle RA and Rajkumar SV. Prevalence and monitoring of oligosecretory myeloma. N Engl J Med 2012; 367: 580-581.

[8] Ayliffe MJ, Davies FE, de Castro D and Morgan GJ. Demonstration of changes in plasma cell subsets in multiple myeloma. Haematologica 2007; 92: 1135-1138.

[9] Hobbs JA, Drayson MT, Sharp K, Harding S, Bradwell AR and Mead GP. Frequency of altered monoclonal protein production at relapse of multiple myeloma. Br J Haematol 2010; 148: 659-661.

[10] Ritts RE Jr, Ruiz-Argüelles A, Weyl KG, Bradley AL, Weihmeir B, Jacobsen DJ and Strehlo BL. Establishment and characterization of a human non-secretory plasmacytoid cell line and

its hybridization with human B cells. Int J Cancer 1983; 31: 133-141.
[11] Ohtsuki T, Yawata Y, Wada H, Sugihara T, Mori M and Namba M. Two human myeloma cell lines, amylase-producing KMS-12-PE and amylase-non-producing KMS-12-BM, were established from a patient, having the same chromosome marker, t(11;14)(q13;q32). Br J Haematol 1989; 73: 199-204.
[12] Kubonishi I, Seto M, Shimamura T, Enzan H and Miyoshi I. The establishment of an interleukin-6-dependent myeloma cell line (FLAM-76) carrying t(11;14)(q13;q32) chromosome abnormality from an aggressive nonsecretory plasma cell leukemia. Cancer 1992; 70: 1528-1535.
[13] Ri M, Iida S, Nakashima T, Miyazaki H, Mori F, Ito A, Inagaki A, Kusumoto S, Ishida T, Komatsu H, Shiotsu Y and Ueda R. Bortezomib-resistant myeloma cell lines: a role for mutated PSMB5 in preventing the accumulation of unfolded proteins and fatal ER stress. Leukemia 2010; 24: 1506-1512.
[14] Zi FM, He JS, Li Y, Wu C, Wu WJ, Yang Y, Wang LJ, He DH, Yang L, Zhao Y, Zheng GF, Han XY, Huang H, Yi Q and Cai Z. Fibroblast activation protein protects bortezomib-induced apoptosis in multiple myeloma cells through β-catenin signaling pathway. Cancer Biol Ther 2014; 15: 1413-1422.
[15] Saito I, Servenius B, Compton T and Fox RI. Detection of Epstein-Barr virus DNA by polymerase chain reaction in blood and tissue biopsies from patients with Sjogren's syndrome. J Exp Med 1989; 169: 2191-2198.
[16] Nishizono I, Iida S, Suzuki N, Kawada H, Murakami H, Ashihara Y and Okada M. Rapid and sensitive chemiluminescent enzyme immunoassay for measuring tumor markers. Clin Chem 1991; 37: 1639-1644.
[17] Sinclair D, Kumararatne DS and Stott D. Detection and identification of serum monoclonal immunoglobulin by immunoisoelectric focusing. Limits of sensitivity and use during relapse of multiple myeloma. J Clin Pathol 1984; 37: 255-262.
[18] Harada H, Kawano MM, Huang N, Harada Y, Iwato K, Tanabe O, Tanaka H, Sakai A, Asaoku H and Kuramoto A. Phenotypic difference of normal plasma cells from mature myeloma cells. Blood 1993; 81: 2658-2663.
[19] Robillard N, Avet-Loiseau H, Garand R, Moreau P, Pineau D, Rapp MJ, Harousseau JL and Bataille R. CD20 is associated with a small mature plasma cell morphology and t(11;14) in multiple myeloma. Blood 2003; 102: 1070-1071.
[20] Pellat-Deceunynck C, Barillé S, Puthier D, Rapp MJ, Harousseau JL, Bataille R and Amiot M. Adhesion molecules on human myeloma cells: significant changes in expression related to malignancy, tumor spreading, and immortalization. Cancer Res 1995; 55: 3647-3653.
[21] Nahi H, Sutlu T, Jansson M, Alici E and Gahrton G. Clinical impact of chromosomal aberrations in multiple myeloma. J Intern Med 2011; 269: 137-147.
[22] Grzasko N, Hus M, Pluta A, Jurczyszyn A, Walter-Croneck A, Morawska M, Chocholska S, Hajek R and Dmoszynska A. Additional genetic abnormalities significantly worsen poor prognosis associated with 1q21 amplification in multiple myeloma patients. Hematol Oncol 2013; 31: 41-48.
[23] Sawyer JR, Waldron JA, Jagannath S and Barlogie B. Cytogenetic findings in 200 patients with multiple myeloma. Cancer Genet Cytogenet 1995; 82: 41-49.
[24] Kühnemund A, Liebisch P, Bauchmüller K, zur Hausen A, Veelken H, Wäsch R and Engelhardt M. 'Light-chain escape-multiple myeloma'-an escape phenomenon from plateau phase: report of the largest patient series using LC-monitoring. J Cancer Res Clin Oncol 2009; 135: 477-484.
[25] Cogné M and Guglielmi P. Exon skipping without splice site mutation accounting for abnormal immunoglobulin chains in nonsecretory human myeloma. Eur J Immunol 1993; 23: 1289-1293.
[26] Dul JL and Argon Y. A single amino acid substitution in the variable region of the light chain specifically blocks immunoglobulin secretion. Proc Natl Acad Sci U S A 1990; 87: 8135-8139.
[27] Pellat-Deceunynk C, Amiot M, Bataille R, Van Riet I, Van Camp B, Omede P and Boccadoro M. Human myeloma cell lines as a tool for studying the biology of multiple myeloma: a reappraisal 18 years after. Blood 1995; 86: 4001-4002.
[28] Park J, Bae EK, Lee C, Choi JH, Jung WJ, Ahn KS and Yoon SS. Establishment and characterization of bortezomib-resistant U266 cell line: constitutive activation of NF-κB-mediated cell signals and/or alterations of ubiquitylation-related genes reduce bortezomib-induced apoptosis. BMB Rep 2014; 47: 274-279.
[29] Song IS, Kim HK, Lee SR, Jeong SH, Kim N, Ko KS, Rhee BD and Han J. Mitochondrial modulation decreases the bortezomib-resistance in multiple myeloma cells. Int J Cancer 2013; 133: 1357-1367.
[30] Song IS, Jeong YJ, Jeong SH, Heo HJ, Kim HK, Lee SR, Ko TH, Youm JB, Kim N, Ko KS, Rhee

BD and Han J. Combination treatment with 2-methoxyestradiol overcomes bortezomib resistance of multiple myeloma cells. Exp Mol Med 2013; 45: e50.

[31] Wong KY, Wan TS, So CC and Chim CS. Establishment of a bortezomib-resistant Chinese human multiple myeloma cell line: MMLAL. Cancer Cell Int 2013; 13: 122.

[32] Markovina S, Callander NS, O'Connor SL, Kim J, Werndli JE, Raschko M, Leith CP, Kahl BS, Kim K and Miyamoto S. Bortezomib-resistant nuclear factor-kappaB activity in multiple myeloma cells. Mol Cancer Res 2008; 6: 1356-1364.